IBIS 2.0

Conceptual design of the IBIS 2.0 polarimetric unit

Document number: IBIS-TRE-01

Document version: 2.0

Released on: 2022-02-12

Prepared by: Giorgio Viavattene

Authors

Name	Affiliation
Runa Briguglio	INAF - OAA
Fabrizio Giorgi	INAF - OAR
Maurizio Oliviero	INAF - OAC
Fernando Pedichini	INAF - OAR
Alessandro Terreri	INAF - OAR
Giorgio Viavattene	INAF - OAR

Change record from previous version

Affected section(s)	Changes / Reason / Remarks
All	Updates after review for submission to INAF Open Access repository.

Contents

1 Introduction

1.1 Purpose

This document describes the optical and polarimetric design of the polarimetric unit of the Interferometric BIdimensional Spectrometer (IBIS) 2.0 instrument, which will be used at the German Vacuum Tower Telescope (VTT) to acquire high resolution spectro-polarimetric observations. The design has been implemented following the scheme of the previous polarimeter of IBIS used at the Dunn Solar Telescope (DST).

1.2 Definitions, acronyms and abbreviations

AO	Adaptive Optics
CAM	Camera sensor
CCD	Charge-Coupled Device sensor
DST	Dunn Solar Telescope
FLC	Ferroelectric Liquid Crystal
FS	Field Stop
FoV	Field of View
FW	Filter Wheel
IBIS	Intereferometric BIdimensional Spectrometer
ICU	Instrument Calibration Unit
IDL	Interactive Data Language
KAOS	Kiepenheuer-institute Adaptive Optic System
L	Lens
LCVR	Liquid Crystal Variable Retarder
M, m	Mirror
PBS	Polarizing Beam Splitter
RL	Relay Lens
VTT	Vacuum Tower Telescope

Acknowledgements: Authors thanks Dr. Matteo Munari of INAF – Astrophysical Observatory of Catania, and Dr. Federico Landini of INAF – Astrophysical Observatory of Turin for the referee process of this document.

2 Related documents

RD1 IBIS at DST: Optomechanical Layout and Instrument Control (IBIS-05)

RD2 System Design Description (IBIS-04)

RD3 IBIS Data Reduction Notes by S. Criscuoli and A. Tritschler

3 Polarimetry with IBIS at DST

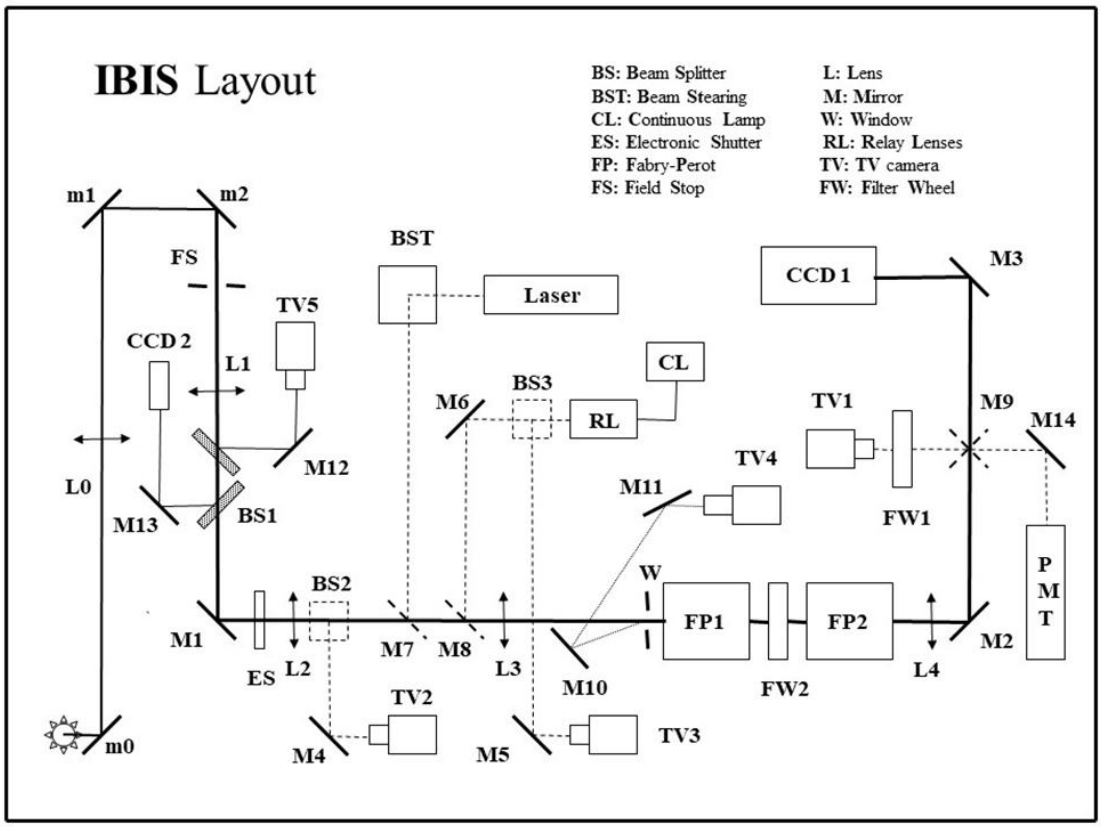

Figure 1: Optical scheme of IBIS at DST.

Since 2006, IBIS (Cavallini 2006) has been used to acquire high resolution spectro-polarimetric data at the DST using a polarimeter based on two Liquid Crystal Variable Retarders (LCVRs) and a Polarizing Beam Splitter (PBS) [RD1]. The optical scheme of IBIS at DST is reported in Figure 1. To perform spectro-polarimetric observations, some manual instrumental changes were done: the circular Field Stop (FS), producing a Field-of-View (FoV) of 80”, was substituted with a rectangular one, producing a halved FoV of 40”x80”; the LCVRs placed between m0 and L0 were activated; L4 and CCD1 were moved 12 cm forward and the PBS was inserted between M3 and CCD1. The PBS split the light beam into two vertical rectangular images on CCD1, which had linear polarization mutually perpendicular to each other. After their voltages calibration, the LCVRs were used to obtain the following six modulation states on the left vertical rectangular image on CCD1 (the right vertical rectangular image had the inverted sign): I+Q, I+V, I-Q, I-V, I-U, I+U. This modulation order has been optimized in order to have the fastest acquisition scheme since the retardance rise time of the LCVRs is longer than the retardance fall time. The six modulation states were converted in the four Stokes parameters I, Q, U and V by the data calibration pipeline [RD3]. Recalling that the two LCVRs were mounted with their fast axis at 45° one with respect to the other, the retardance of the two LCVRs for each modulation state (data found in the header of the raw files) are reported in Table 1:

Modulation state	LCVR 1 retardance [deg]	LCVR 1 retardance [wave]	LCVR 2 retardance [deg]	LCVR 2 retardance [wave]
I+Q	360	λ	360	λ
I+V	360	λ	270	¾ λ
I-Q	360	λ	180	λ/2
I-V	360	λ	90	λ/4
I-U	270	¾ λ	90	λ/4
I+U	90	λ/4	90	λ/4

Table 1: : Modulation states and LCVRs retardances for IBIS polarimeter used at DST. The same modulation states will be used for the IBIS 2.0 polarimeter at VTT.

4 Polarimetry with IBIS 2.0 at VTT

IBIS 2.0 will be used to perform high resolution spectro-polarimetric observations at the VTT in a similar way to what done at the DST [RD2]. Therefore, the IBIS 2.0 polarimeter has been designed through a combination of a reverse engineering process of the previous IBIS polarimeter used at DST and a more modern optical design and optimization using OpticStudio (Zemax) software.

Table 2 reports the instrumental requirements for the IBIS 2.0 polarimeter. In order to reduce the number of actuators/stages, the PBS can be placed in the Filter Wheel 1 (FW1), which is placed before CAM1 [RD2]. Therefore, the available space for the PBS is the dimension of a single slot of the FW1.

Item	Requirement
FoV [arcsec^2]	80x80
Distance between the two split images' centers [mm]	~ 6.65
Image dimension in spectroscopic mode [mm]	~ 5.69
Beam diameter in the polarimetric modulator place [mm]	< 50
Available space for the PBS (LxWxH) [mm]	45x18x18

Table 2: Instrumental requirements of the IBIS 2.0 polarimeter.

During the polarimeter design process, several designs of other solar polarimeters have been studied in order to identify the best feasible solution for the IBIS 2.0 polarimeter (Schurcliff 1962, Collados 2007a, Keller, del Toro Iniesta 2003).

Polarimeters with rotating retarder are no longer realized due to their long acquisition time (Lites 1987, Schmidt et al. 2001, Beck 2002). In the last two decades, solar polarimeters have been realized using dual-beam polarimetry (on either one or two detectors) by employing a PBS as a *polarimetric analyzer* and a set of two LCVRs or two Ferroelectric Liquid Crystals (FLCs) as a *polarimetric modulator* placed before the PBS (Collados 1999, Collados 2007a, del Toro Iniesta 2003). The LCVRs are optical devices whose retardances can be varied by voltages changes and they are mounted with a fixed orientation angle; conversely the FLCs are optical devices realized with fixed retardances and their orientation angle can be varied by voltages changes.

There are also several polarimetric modulation schemes used in solar polarimeters recently developed: producing e.g. six states with two LCVRs in IBIS (Cavallini 2006), four states with two LCVRs in TESOS (Beck et al. 2010), four states with two FLCs (Gandorfer 1999, Bello Gonzalez and Kneer 2008, Martinez Pillet et a. 1999) in LPSP and TIP. The PBS has been usually realized with a Wollaston prism (Beck et al. 2010), a modified Savart plate (Bello Gonzalez and Kneer 2008), a set of cemented polarizing cube beam splitters (Collados et al. 2007b), and a cube beam splitter which sends the light in two detectors like in CRISP (Scharmer 2006).

The choice to design a polarimeter similar to the one used at DST has been driven by the following reasons:

- The IBIS 2.0 Team has a solid expertise in calibrating and analyzing this kind of spectro-polarimetric data.
- The already developed calibration pipeline of IBIS [RD3] can be reused for IBIS 2.0 with only minor changes.
- Several instrumental data have been found in the header of the files acquired with IBIS at DST, helping the reverse engineering process.
- The strategic modulation scheme based on six modulation states allows to have data with reduced cross-talk between the Stokes parameters (since the modulation states are a linear combination of Stokes parameters with integer coefficients) with considerably higher efficiency of the modulation scheme (Collados 1999, Collados 2007a, del Toro Iniesta and Collados 2000) than other schemes.

- The combination of spatial and temporal modulation allows to reduce the seeing-induced cross-talk and the gain-table uncertainties, respectively (Collados 1999).
- The use of a PBS before the scientific detector allows to perform dual-beam polarimetry, imaging the split beam in the same detector, therefore reducing the polarimetric uncertainties and simplifying the calibration pipeline, besides of a halved cost of requiring a single detector.
- The LCVRs are placed near a pupil plane (not exactly in the pupil plane, to avoid problems due to the optical quality of the LCVRs) and far away from an image plane in order to prevent them from heating problems.
- Largely tested voltages calibration scheme of the LCVRs and polarimetric calibration scheme of the whole instrument.

Figure 2 shows the optical relay system between the telescope focus and the IBIS 2.0 FS; the two LCVRs are inserted at ~150-200 mm from the pupil plane between RL1 and RL2. Figure 3 shows the optical layout of IBIS 2.0; the PBS will be located before the scientific camera CAM1.

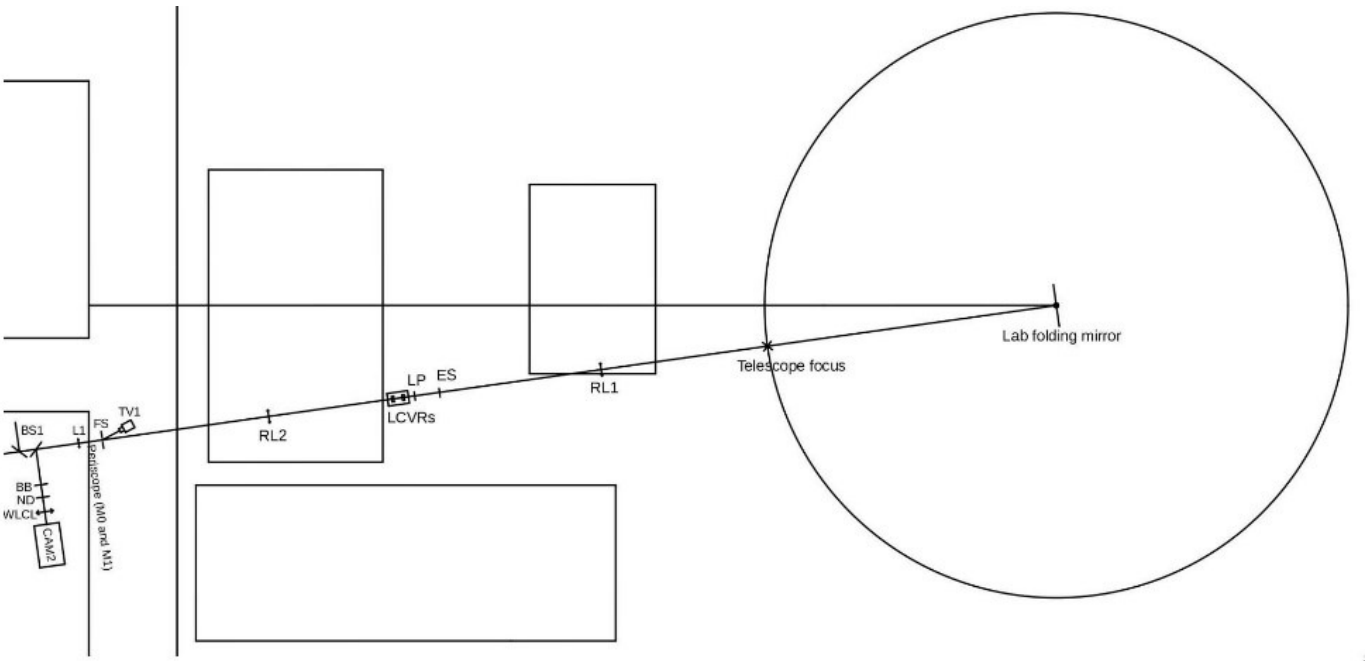

Figure 2: Optical relay system between the telescope focus and the IBIS 2.0 FS, showing the position of the two LCVRs. The rectangles are the optical tables, the circle indicates the position of the telescope focus rotatable with the Lab folding mirror.

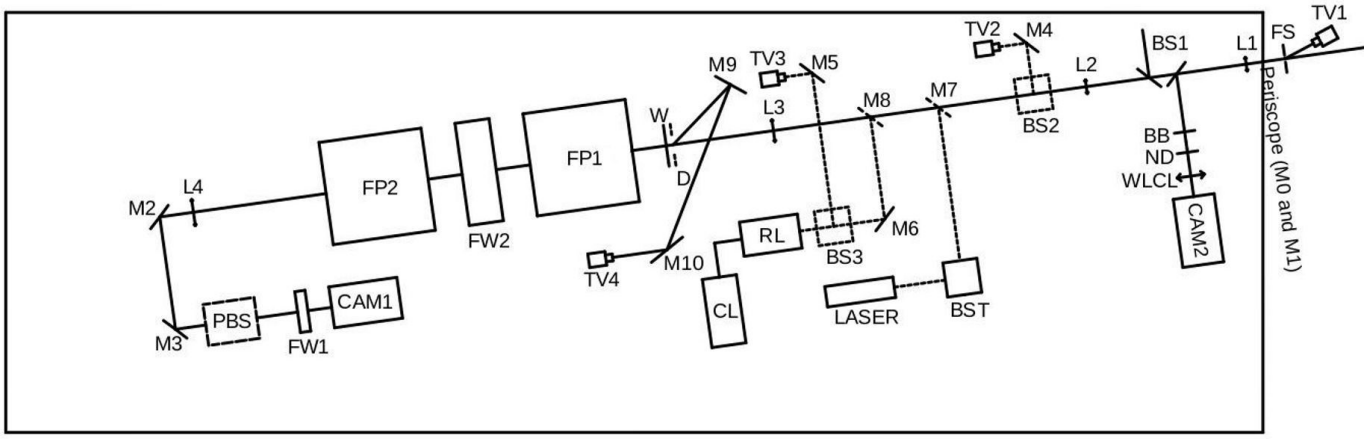

Figure 3: Optical layout of IBIS 2.0, showing the position of the PBS. The rectangle is the optical table above which the instrument will be mounted at VTT.

5 Modulation strategy and calibration of the IBIS 2.0 polarimeter at VTT

5.1 Modulation strategy with two LCVRs and one PBS

As stated before, the module with the two LCVRs will be placed approximately 150-200 mm away from the pupil (approximately 15 mm in diameter) between the two relay lenses, which are used to transfer telecentrically the image of the telescope primary focus on the IBIS 2.0 FS. A UV-cut filter (< 450 nm) will be placed in front of the LCVRs module to protect them from UV damages.

Despite the LCVRs have a longer setting time (milliseconds) with respect to the FLCs (microseconds), they have been preferred for the IBIS 2.0 polarimeter because they can be used in larger wavelength ranges (IBIS 2.0 wavelength range being 580-860 nm) while the FLCs have a good transparency and contrast in a limited wavelength range of at maximum 100 nm. The clear aperture of the LCVRs should be of the order of 20 mm in order not to vignetting the pupil between the two relay lenses. In addition, the LCVRs must be temperature-stabilized (±1°C) since their retardance depends on temperature.

The modulation scheme of the IBIS 2.0 polarimeter at VTT will be the same of the IBIS polarimeter at DST. In fact, a modulation strategy based on six modulation states is suitable for the following reasons:

- The LCVRs retardances are all multiples of 90 degrees (corresponding to λ/4) for all the modulation states; therefore, the LCVRs retardance behavior can be checked and tested with λ/2 and λ/4 retarders and linear polarizers. The use of a modulation scheme based on four states would have required LCVRs retardances not multiples of 90 degrees or angles with decimal digits (Beck et al. 2010), which could be difficult to check and test with ordinary retarders and polarizers.
- The output of the modulation states is a linear combination of Stokes parameters with integer (and not irrational) coefficients: this allows to have a reduced cross-talk between the Stokes parameters, to have a simpler data calibration pipeline and to recover roughly the Stokes parameters through sum and differences of the two images on the scientific detector.
- The polarimetric demodulation routines of the IBIS calibration pipeline used at DST [RD3] do not need to be changed for the calibration pipeline of the IBIS 2.0 polarimeter at VTT.

The modulation scheme of the LCVRs in combination with the PBS has been studied using a code developed with Interactive Data Language (IDL) based on Mueller matrix calculation. When there is more than one optical polarimetric element, the resulting Mueller matrix of the optical train is given by:

$$M_{tot} = M_N \cdot M_{N-1} \cdot \ldots \cdot M_2 \cdot M_1$$

where M_N is the Mueller matrix of the last element and M_1 is the Mueller matrix of the first element. Therefore, the Mueller matrix of the IBIS 2.0 polarimeter is given by:

$$M_{IBIS\_spectropol} = M_{PBS} \cdot M_{LCVR2} \cdot M_{LCVR1}$$

The Mueller matrix of the PBS is the matrix of a linear polarizer with either horizontal (0°) or vertical (90°) orientation for the either left or right split beams, respectively:

$$M_{PBS\_left} = \frac{1}{2}\begin{pmatrix} 1 & 1 & 0 & 0 \\ 1 & 1 & 0 & 0 \\ 0 & 0 & 0 & 0 \\ 0 & 0 & 0 & 0 \end{pmatrix}$$

$$M_{PBS\_right} = \frac{1}{2}\begin{pmatrix} 1 & -1 & 0 & 0 \\ -1 & 1 & 0 & 0 \\ 0 & 0 & 0 & 0 \\ 0 & 0 & 0 & 0 \end{pmatrix}$$

Since the LCVRs are mounted with an orientation angle θ, the general matrix of a retarder (with a retardance δ)

$$M_{ret} = \begin{pmatrix} 1 & 0 & 0 & 0 \\ 0 & 1 & 0 & 0 \\ 0 & 0 & \cos\delta & -\sin\delta \\ 0 & 0 & \sin\delta & \cos\delta \end{pmatrix}$$

must be rotated using the rotation matrix with the following relation:

$$M_{LCVR} = R(-\theta) \cdot M_{ret} \cdot R(\theta) = \begin{pmatrix} 1 & 0 & 0 & 0 \\ 0 & c_2 & -s_2 & 0 \\ 0 & s_2 & c_2 & 0 \\ 0 & 0 & 0 & 1 \end{pmatrix} \cdot \begin{pmatrix} 1 & 0 & 0 & 0 \\ 0 & 1 & 0 & 0 \\ 0 & 0 & \cos\delta & -\sin\delta \\ 0 & 0 & \sin\delta & \cos\delta \end{pmatrix} \cdot \begin{pmatrix} 1 & 0 & 0 & 0 \\ 0 & c_2 & s_2 & 0 \\ 0 & -s_2 & c_2 & 0 \\ 0 & 0 & 0 & 1 \end{pmatrix}$$

where $c_2 = \cos(2\theta)$ and $s_2 = \sin(2\theta)$.

Calculating the matrix $M_{IBIS\_spectropol}$ and replacing the LCVRs retardance angles listed in Table 1, the simulation has been used to determine the orientation angle of the two LCVRs in order to obtain the correct modulation states with the respective LCVRs retardances. The result is that the orientation angles are 90° and 135° for LCVR1 and LCVR2, respectively.

5.2 LCVRs voltages calibration with the Calibration Linear Polarizer

The LCVRs of the IBIS 2.0 polarimeter must be calibrated before each observing run, in order to associate the voltages applied to them with the corresponding retardances, since their relation varies with respect to the wavelength, temperature and other factors (telescope misalignments, beam wobble, deterioration of liquid crystals, etc.). Therefore, this calibration must be repeated for each observed wavelength during the observing campaign, since the experience with IBIS at DST has shown that this calibration is fundamental to reduce the cross-talks between the Stokes profiles and to reach the polarimetric sensitivity of 10^{-3} expected by the instrument.

As previously done with the IBIS polarimeter used at DST, this procedure involves the use of a calibration linear polarizer inserted before the LCVRs module during the calibration phase. In this case, the Mueller matrix of the polarimetric train is given by:

$$M_{IBIS\_spectropol\_cal} = M_{PBS} \cdot M_{LCVR2} \cdot M_{LCVR1} \cdot M_{cal\_lin\_pol}$$

where M_{PBS} and M_{LCVR} are the same matrices presented above and

$$M_{cal\_lin\_pol} = \frac{1}{2} \begin{pmatrix} 1 & c_2 & s_2 & 0 \\ c_s & c_2^2 & c_2 s_2 & 0 \\ s_2 & c_2 s_2 & s_2^2 & 0 \\ 0 & 0 & 0 & 0 \end{pmatrix}$$

is the Mueller matrix of the calibration linear polarizer with a general orientation angle θ of its transmission axis.

The two LCVRs are calibrated separately. Our calculations with Mueller matrices aim to find the orientation angles of the transmission axis of the calibration linear polarizer during the calibration of the two LCVRs, respectively.

The calibration steps are:

1. Firstly, the LCVR 2 is calibrated (while the LCVR 1 is set at 0λ retardance) by inserting the calibration linear polarizer with an orientation angle of 90° and sending on LCVR 2 an increasing and decreasing voltage signal. In this case, considering the whole polarimetric train, the output seen by CAM1 is the following:
    A. Left and right images with the same (halved) intensity: the LCVR 2 has a retardance of λ/4 and it produces a right circular polarized light (in combination with the calibration linear polarizer), which is equally divided on CAM1 by the PBS;
    B. Left image luminous and right image dark: the LCVR 2 has a retardance of λ/2 and it produces a horizontal linear polarized light (in combination with the calibration linear

polarizer), which is completely transmitted in the left beam and completely blocked in the right beam produced by the PBS on CAM1;

C. Left and right images with the same (halved) intensity: the LCVR 2 has a retardance of 3λ/4 and it produces a left circular polarized light (in combination with the calibration linear polarizer), which is equally divided on CAM1 by the PBS;

D. Left image dark and right image luminous: the LCVR 2 has a retardance of λ and it produces a vertical linear polarized light (in combination with the calibration linear polarizer), which is completely blocked in the left beam and completely transmitted in the right beam produced by the PBS on CAM1.

The ambiguity between case A. and case C. is removed by considering the increasing and decreasing voltage signal applied on LCVR 2. A scheme of this calibration for LCVR 2 is shown in Figure 4:

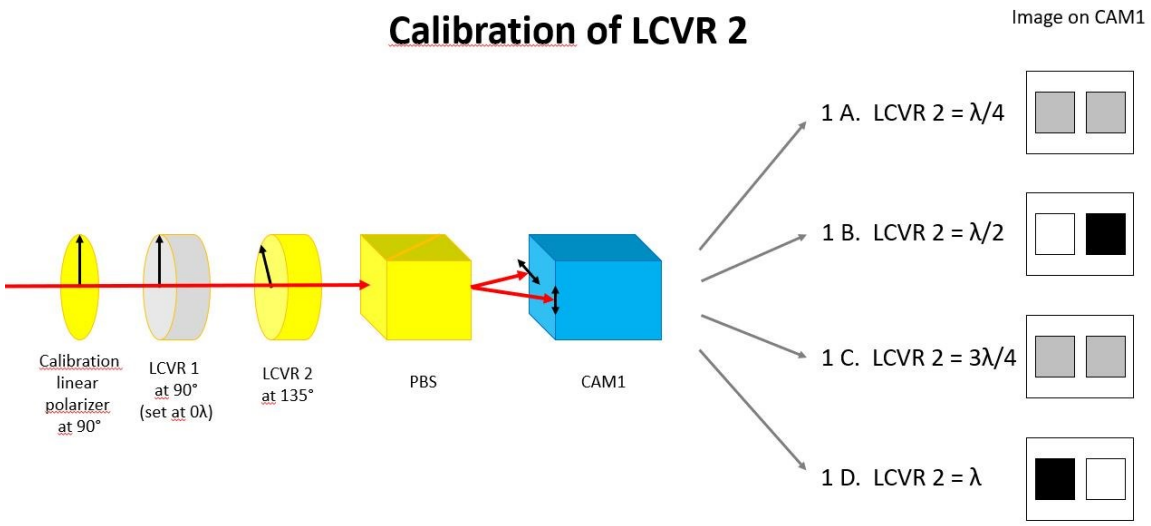

Figure 4: Calibration scheme of LCVR 2.

2. Secondly, the LCVR 1 is calibrated (while the LCVR 2 is set with a retardance of λ/4) by inserting the calibration linear polarizer with an orientation angle of 45° and sending on LCVR 1 an increasing and decreasing voltage signal. In this case, considering the whole polarimetric train, the output seen by CAM1 is the following:
   A. Left image luminous and right image dark: the LCVR 1 has a retardance of λ/4 and it produces a horizontal linear polarized light (in combination with the calibration linear polarizer and with the LCVR 2 set at λ/4), which is completely transmitted in the left beam and completely blocked in the right beam produced by the PBS in CAM1;
   B. Left and right images with the same (halved) intensity: the LCVR 1 has a retardance of λ/2 and it produces a linear polarized light at 135° (in combination with the calibration linear polarizer and with the LCVR 2 set at λ/4), which is equally divided on CAM1 by the PBS;
   C. Left image dark and right image luminous: the LCVR 1 has a retardance of 3λ/4 and it produces a vertical linear polarized light (in combination with the calibration linear polarizer and with the LCVR 2 set at λ/4), which is completely blocked in the left beam and completely transmitted in the right beam produced by the PBS in CAM1;
   D. Left and right images with the same (halved) intensity: the LCVR 1 has a retardance of λ and it produces a linear polarized light at 45° (in combination with the calibration linear polarizer and with the LCVR 2 set at λ/4), which is equally divided on CAM1 by the PBS.

The ambiguity between case B. and case D. is removed by considering the increasing and decreasing voltage signal applied on LCVR 1. A scheme of this calibration for LCVR 1 is shown in Figure 5:

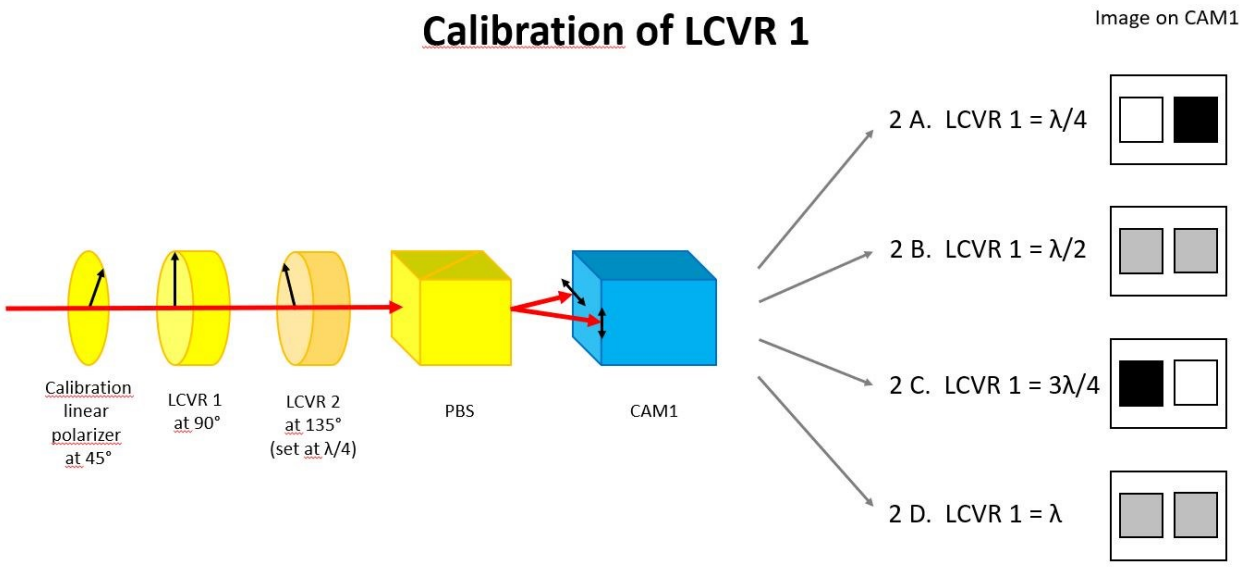

Figure 5: Calibration scheme of LCVR 1.

5.3 IBIS 2.0 polarimetric calibration at VTT with the ICU and the telescope model

The polarimetric data must be corrected for the influence of the telescope and the instrument itself. The measured Stokes vector S_{out} is related with the incoming Stokes vector from the Sun S_{in} by the following equation:

$$S_{out} = X \cdot T \cdot S_{in}$$

where X is the Mueller matrix of the polarimetric response of the instrument itself (the so-called X-matrix) and T is the Mueller matrix of the polarimetric response of the telescope (the so-called T-matrix). The Stokes vector S_{in} coming from the Sun is recovered by inverting the above equation having measured the Stokes vector S_{out}. The X-matrix describes the polarimetric behavior of all the optical elements placed after the ICU; the T-matrix describes the polarimetric behavior of all the optical elements placed before the ICU.

We decided to follow the same strategy used with IBIS at DST to evaluate the X-matrix of IBIS 2.0 at VTT using the Instrument Calibration Unit (ICU). The ICU of the VTT (located inside the vacuum tank, before KAOS, van der Luhe et al. 2003) has the same optical elements of the one used at DST: a linear polarizer and a retarder (approximately a quarter-wave plate).

During the measurements for the evaluation of the X-matrix for IBIS at DST, the linear polarizer and the retarder of the ICU of the DST were inserted into the beam and rotated at various angles in 24 configurations using servomechanisms, as summarized in Table 3. For each configuration of the ICU, the six modulation states were acquired, and this procedure was repeated for each observed wavelength. The IBIS pipeline [RD3] firstly evaluates the theoretical X-matrix for each given configuration and then modifies its terms by interpolating the split images intensities acquired with the science camera CCD1. In this way the polarimetric spurious signals generated by other optical components were included in the X-matrix as the polarimetric response of the instrument to various known polarimetric inputs sent by the ICU (see later).

The difference between the ICU of the DST and the one of the VTT lies in the fact that in the case of the VTT the linear polarizer and the retarder are inserted/removed at the same time in/from the

beam as they are mounted on the same translational stage and they cannot be inserted individually as it was done at the DST. For this reason, the first 8 configurations of Table 3 cannot be performed with the ICU of the VTT. We tested this approach by excluding the first 8 configurations of the ICU running the pipeline of IBIS [RD3] using datasets acquired at DST. We notice that these first 8 configurations were only used to refine the interpolation of the X-matrix terms of the order of 10^{-3}, which is the polarimetric sensitivity of IBIS, and the same variations of the order of 10^{-3} are observed in the maps of the Stokes profiles with respect to the one calibrated using the full set of configurations. The Stokes profiles evaluated with the exclusion of the first 8 configurations are the same (superimposable) of the ones evaluated with the full set of configurations. Therefore, the exclusion of the first 8 configurations will not affect appreciably the polarimetric calibration of the instrument. The ICU of the VTT can be used properly for the polarimetric calibration of IBIS 2.0 setting it at the remaining 16 configurations. The polarimetric calibration routine of the IBIS pipeline at DST will be revised to work with IBIS 2.0 at VTT.

We developed an evaluation code with IDL to test this approach using the Mueller calculus. In this case, when the ICU is activated for the evaluation of the X-matrix, the Mueller matrix of the whole optical train is given by:

$$M_{IBIS\_icu} = M_{PBS} \cdot M_{LCVR2} \cdot M_{LCVR1} \cdot M_{icu\_ret} \cdot M_{icu\_pol}$$

where M_{PBS} and M_{LCVR} are the same matrices described above, and M_{icu_ret} and M_{icu_pol} are the Mueller matrices of the retarder and the polarizer of the ICU, respectively:

$$M_{icu\_ret} = R(-\theta) \cdot M_{ret} \cdot R(\theta) = \begin{pmatrix} 1 & 0 & 0 & 0 \\ 0 & c_2 & -s_2 & 0 \\ 0 & s_2 & c_2 & 0 \\ 0 & 0 & 0 & 1 \end{pmatrix} \cdot \begin{pmatrix} 1 & 0 & 0 & 0 \\ 0 & 1 & 0 & 0 \\ 0 & 0 & \cos\delta & -\sin\delta \\ 0 & 0 & \sin\delta & \cos\delta \end{pmatrix} \cdot \begin{pmatrix} 1 & 0 & 0 & 0 \\ 0 & c_2 & s_2 & 0 \\ 0 & -s_2 & c_2 & 0 \\ 0 & 0 & 0 & 1 \end{pmatrix}$$

with $\delta = 90°$ (quarter-wave plate) and

$$M_{icu\_pol} = \frac{1}{2} \begin{pmatrix} 1 & c_2 & s_2 & 0 \\ c_s & c_2^2 & c_2 s_2 & 0 \\ s_2 & c_2 s_2 & s_2^2 & 0 \\ 0 & 0 & 0 & 0 \end{pmatrix}$$

The evaluation code showed that the strategy with 24 configurations of the ICU perfectly works also for the IBIS 2.0 polarimeter at VTT since we obtain the same polarization signals on the two images on CAM1 as for the polarimeter of IBIS at DST. As stated before, for the evaluation of the IBIS 2.0 X-matrix at VTT only the last 16 configurations of the ICU will be used.

In addition, the matrix M_{IBIS_icu} (shown in the previous section) is the theoretical one considering the acting polarizing optical elements, and therefore it should be equal to the X-matrix. The real measured X-matrix, which results from sending known polarization states on the instrument using the ICU, also contains contribution of other optical elements inside IBIS 2.0 and KAOS, e.g. the optical window W, the mirrors, etc. These could contribute with spurious polarimetric signals that are difficult to model. As stated before, the IBIS pipeline used at DST already takes into account these effects by extracting them from the measured X-matrix, which is interpolated over the theoretical one. The new pipeline of IBIS 2.0 shall maintain these actions for the calibration for the X-matrix; in this way, the polarimetric spurious signal of the other optical elements of IBIS 2.0 and KAOS shall be absorbed in the overall effect of the X-matrix.

Position	Polarizer	Polarizer angle [deg]	Retarder	Retarder angle [deg]
1	Out	0	In	0
2	Out	0	In	45
3	Out	0	In	90
4	Out	0	In	135
5	In	0	Out	0
6	In	45	Out	0
7	In	90	Out	0
8	In	135	Out	0
9	In	0	In	0
10	In	0	In	45
11	In	0	In	90
12	In	0	In	135
13	In	45	In	180
14	In	45	In	225
15	In	45	In	270
16	In	45	In	315
17	In	90	In	0
18	In	90	In	45
19	In	90	In	90
20	In	90	In	135
21	In	135	In	180
22	In	135	In	225
23	In	135	In	270
24	In	135	In	315

Table 3: Positions and angles of the linear polarizer and of the retarder of the ICU of the DST for the evaluation of the polarimetric X-matrix of IBIS. The first eight rows will not perform with the ICU of the VTT since the polarizer and the retarder are mounted in the same translational stage (see text).

On the other hand, the T-matrix takes into account all the polarimetric spurious signals originated in the telescope optics, such as the ones from reflections on the mirrors (with their inclination angles) and by the tension on the vacuum windows, which are the optics before the ICU. Following the notation of Figure 6, in Beck 2002 and in Beck 2005a, a telescope model for the VTT has been developed using Mueller calculus:

$$T = W_{E2} \cdot R(\theta_4) \cdot M_{M4} \cdot M_{M3} \cdot W_{E1} \cdot R(\theta_3) \cdot M_{C2} \cdot R(\theta_2) \cdot M_{C1} \cdot R(\theta_1)$$

where $R(\theta)$ are the matrices referred to the rotation of the reference frames between subsequent optical elements, W are the Mueller matrices of the vacuum-stressed windows and M are the Mueller matrices of the mirrors. Therefore, the T-matrix strongly depends on the geometry of the beam (the incidence angles on the mirrors and the rotation angles of the various optical elements), on the material properties (refraction indices and extinction coefficients of the mirrors, effective phase shift and angle of the optical axis of the windows). This telescope model is improved performing

instrumental measurements mounting an array of linear polarizers in front of the telescope entrance window E1 or in front of the first coelostat mirror C1. It is worth noting that the T-matrix should be provided by the VTT and it is mandatory for the polarimetric calibration of IBIS 2.0. For other details see the original papers (Beck 2002, Beck et al. 2005b).

The contribution of the two mirrors C1 and C2 of the coelostat can be evaluated using the IDL code *vtt.pro* provided by Manolo Collados (private communication). This code evaluates the Mueller matrix of the two coelostat mirrors using the following inputs: year, month, day and hour of observation, the angle γ of the mirror C1 (see Figure 6) around the telescope tube and the height of the mirror C2 (directly read on the ruler or calculated using another routine of the VTT package). The code evaluates the position of the Sun in the sky using the date and the time of observation, and the altitude and coordinates of the VTT. Then, the code calculates the Mueller matrices of the coelostat mirrors from their optical properties (complex index of refraction and angle of incidence) and generates the total Mueller matrix of the coelostat taking into account its geometry (angles, heights and distances).

The polarimetric signal introduced by the telescope mirrors M3 and M4 is negligible since their inclination angle is 0.84°.

The two telescope vacuum windows E1 and E2 produce a polarimetric signal due to the tension on their surfaces generated by the vacuum pression. According to Beck et al. 2005b, they behave altogether as a slow retarder with a retardance of 3° and an orientation angle that varies from 0° to 20° from 08:00 in the morning and 20:00 in the evening. This behavior is typically measured using the array of linear polarizers mounted in front of the telescope entrance window E1, and it must be measured again before the IBIS 2.0 installation since the vacuum window E1 has been changed with respect to the one used in Beck et al. 2005b.

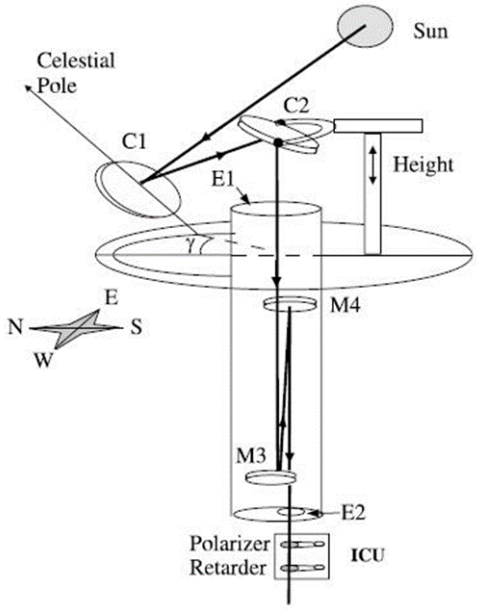

Figure 6: Geometry of the VTT coelostat and telescope vacuum tube.

6 PBS optical design

6.1 PBS alternatives

To perform dual-beam spectro-polarimetry, a PBS must be used before the scientific detector(s). There are several alternatives used in the past in various solar spectro-polarimetric instruments. These are:

- Wollaston prism: it consists of two orthogonal prisms of birifrangent crystal (typically quartz or calcite) which are cemented together on their base to form two right triangle prisms with perpendicular optical axis; the outgoing split beams have perpendicular linear polarization. The Wollaston prisms has been used in TESOS (Beck et al. 2010) and most likely also in the polarimeter of IBIS at DST.
- Modified Savart Plate: it is made by two calcite cubes with their fast axis in the same plane and with a λ/2 retarder (with an orientation angle of 45°) in between them; the λ/2 allows to exchange the ordinary and the extraordinary beams in order to introduce the same astigmatism on both beams after the Modified Savart Plate, since the calcite introduces the astigmatism only on the extraordinary beam. It has been used in the instrument presented by Bello Gonzalez and Kneer 2008.
- Set of cemented polarizing cube beam splitters: this solution has been used for the TIP instrument (Collados et al. 2007b); it consists on an assembly of five cemented prisms, which are used to separate the light in two beams with orthogonal linear polarization and to make the two beams travel the same path, thus avoiding focusing problems.
- Single polarizing cube beam splitter: this is the simplest solution, a cube beam splitter separates the light in two different detectors, as it is done in CRISP (Scharmer 2006).

The single polarizing cube beam splitter has been discarded in the design phase since it requires two scientific detectors and this would strongly impact the costs and the calibration pipeline, since the detector calibration (dark, flat, gain) should be done separately for each detector.

The set of cemented polarizing cube beam splitter has also been discarded due to geometrical problem; in fact, the dimension of the assembly does not fit with the beam dimension and the dimension of the chip of the scientific detector selected for the IBIS 2.0.

After an OpticStudio analysis, the Modified Savart Plate has been rejected since it requires considerably longer calcite crystals to obtain the correct beam separation on the scientific detector. In addition, it is made of three polarimetric elements (two calcites and one λ/2 at 45°) which could be difficult to align. Moreover, the several optical surfaces could cause problems with ghosts and spurious reflections.

The best candidate resulted to be the Wollaston prism. The advantage is that the splitting angle can be regulated by varying the cutting angle of the two prisms which made the Wollaston prism, in order to send both beams on the same detector. Besides, it is only one polarimetric element, which is easier to align and there are only two optical surfaces. The disadvantage of this solution is that the Wollaston prisms must be used in collimated beam otherwise the emerging split beams are affected by different amount of spherical aberration and astigmatism, which cannot be compensated with the same lens. Since the IBIS 2.0 PBS is placed in the converging beam coming from L4, it must require a corrective lenses system to place it in a collimated beam.

6.1.1 Quartz and Calcite Wollaston prism design

Initially, the single Wollaston prism has been studied with OpticStudio software, placed in the convergent beam generated by L4 and just before the CAM1. Both solutions with quartz and calcite have been analyzed, in order to identify the crystal type that produces the correct beam separation with reasonable optical crystal thickness. The calcite produces a larger beam separation due to its larger birefringence with respect to the quartz, as shown in Figure 7 and Figure 8, respectively. Since the Zyla 4.2+ detector is 13.3 mm large, the centers of the two split images by the PBS must be at an optimal distance of ~ 6.65 mm, to avoid the overlapping of the two split images and to prevent

them from coming out of the detector. The squared image produced on CAM1 by L4 in spectroscopic mode is ~ 5.69 mm large; in spectro-polarimetric mode the image size should be about the same. From this preliminary analysis, the trade-off is in favor of the calcite. In addition, as stated before, it can be noticed that the Wollaston prism (of any crystal type) placed in the convergent beam produces two beams with different astigmatism and other aberrations that cannot be compensated with the same corrective lens. The bad spot diagrams of these two solutions with the Wollaston of calcite and quartz for the two split beams are shown in Figure 9 and Figure 10, respectively. It can be noticed that the spot diagrams suffer from strong astigmatism and other aberrations (outside the Airy disk) and this behavior moved us to investigate the solution with the Wollaston prism placed in collimated beam.

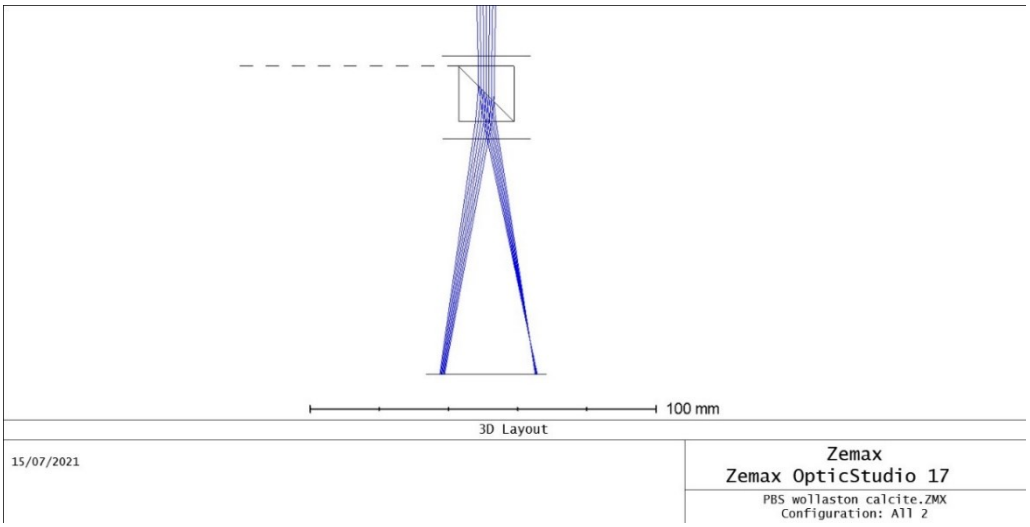

Figure 7: Wollaston prism made of calcite inserted in the convergent beam coming from L4.

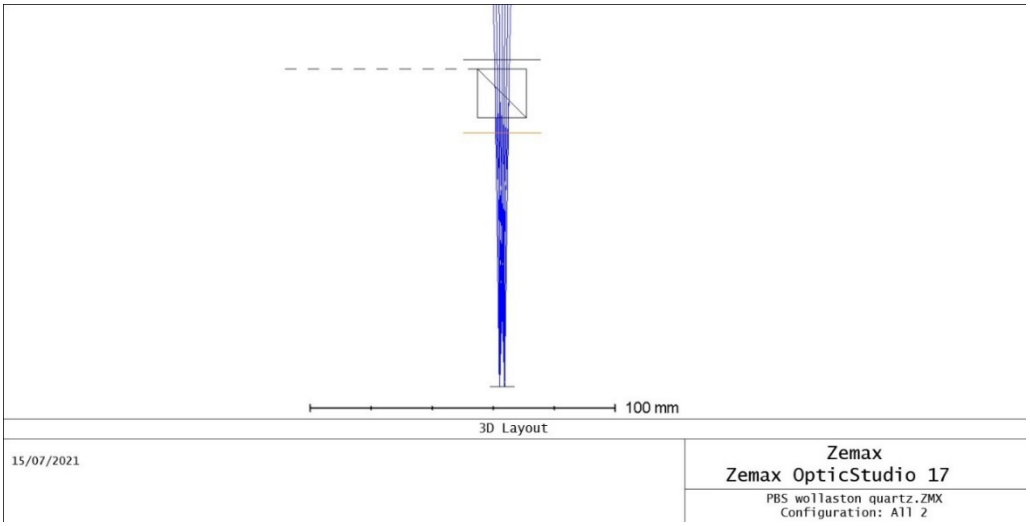

Figure 8: Wollaston prism made of quartz inserted in the convergent beam coming from L4.

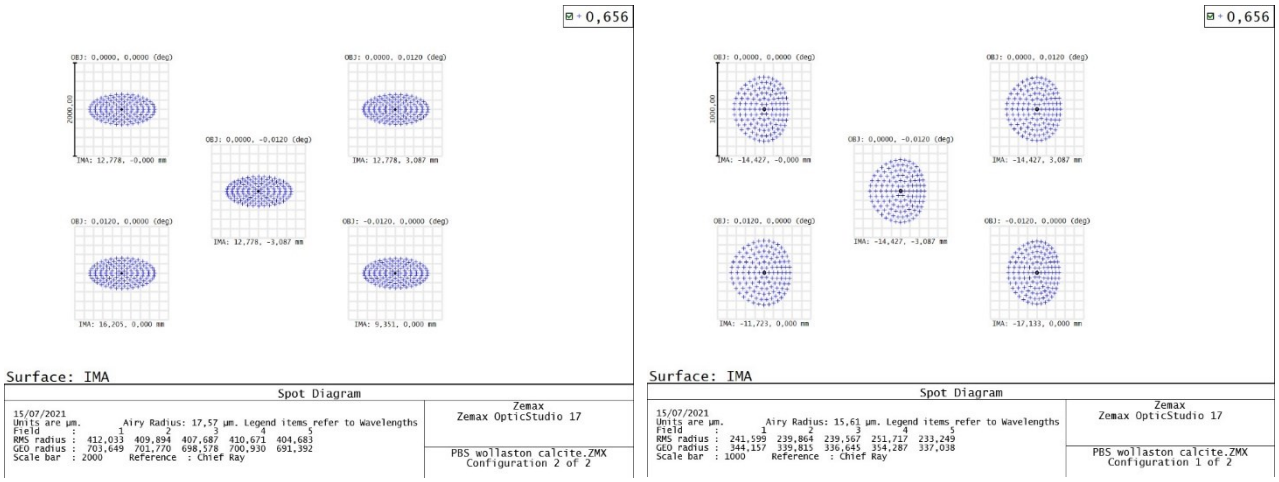

Figure 9: Spot diagrams at 656.3 nm of both the split beams by the Wollaston prism made of calcite placed in the convergent beam coming from L4.

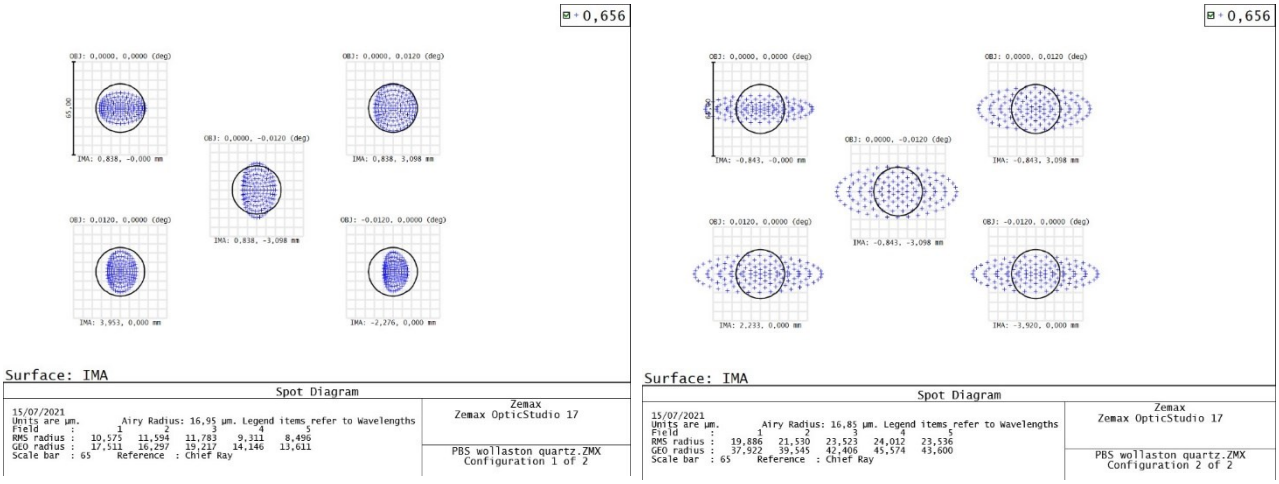

Figure 10: Spot diagrams at 656.3 nm of both the split beams by the Wollaston prism made of quartz placed in the convergent beam coming from L4.

6.1.2 Corrective lenses design

The corrective lenses system serves the purpose of placing the Wollaston prism in a collimated beam, thus using a diverging lens before the prism and a converging lens after it with the same focal length but with opposite sign.

This corrective lenses system has been designed for both the quartz and calcite Wollaston prisms. The solution with the quartz Wollaston prism has been suddenly rejected due to the large thickness of quartz required to obtain the correct beam separation (about 40 mm; note also the large cutting angle) and due to the (oblate or prolate) ovalized Airy disk produced in the two separated beams, as shown in Figure 11 and Figure 12. Therefore, the selected crystal type for the IBIS 2.0 Wollaston prism is made of calcite.

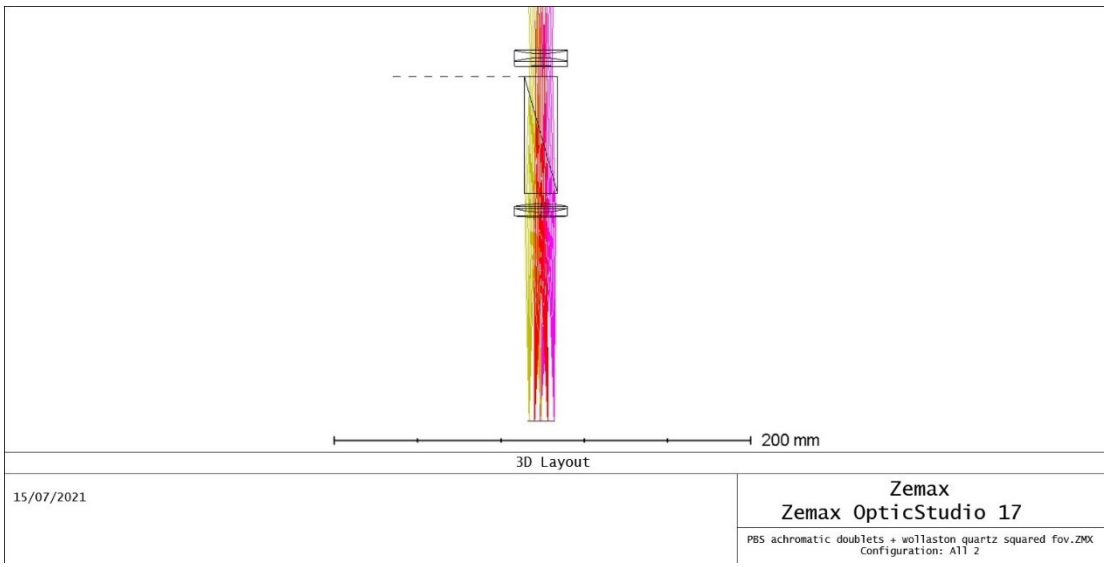

Figure 11: Wollaston prism made of quartz inserted in the collimated beam between the two corrective lenses.

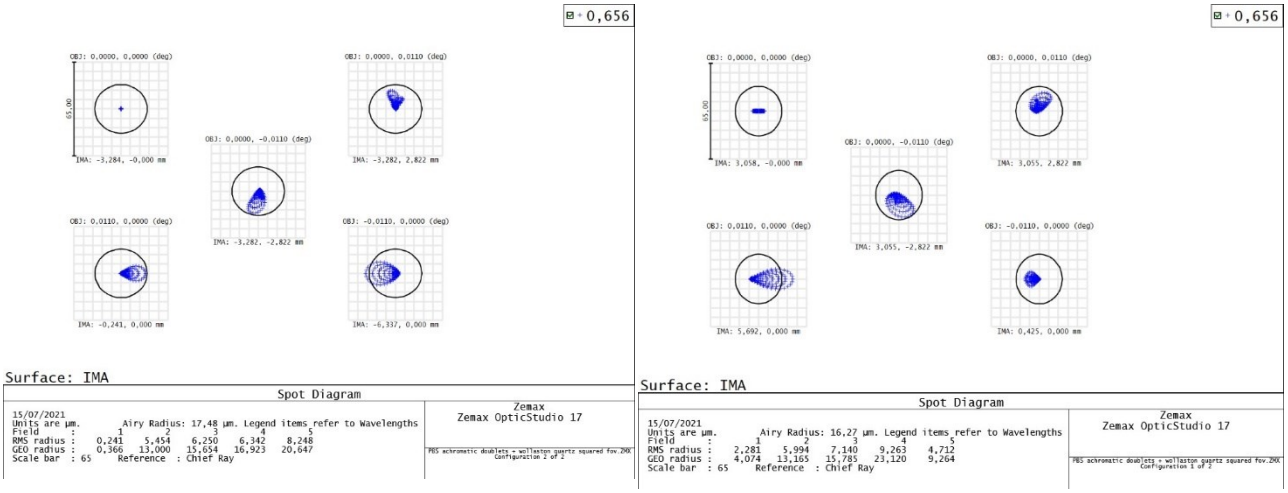

Figure 12: Spot diagrams at 656.3 nm of both the split beams by the Wollaston prism made of quartz placed in the collimated beam between the two corrective lenses

Once decided the type of crystal, two optical designs have been developed with OpticStudio for the corrective lenses system: one based on two achromatic doublets and the other based on two singlet lenses. Both are suitable for the IBIS 2.0 PBS; the choice will be done during a trade-off analysis in the procurement and assembly phases.

Achromatic doublets design

Figure 13 shows the corrective lenses system based on two achromatic doublets and one Wollaston prism made of calcite designed with OpticStudio to fit the IBIS 2.0 PBS requirements. Figure 14 shows the two spot diagrams at 720.0 nm (in the middle of the IBIS 2.0 spectral range) produced by this PBS system (diffraction limited, spots inside the Airy disks). Similar spot diagrams are obtained over the whole spectral range of 580-860 nm. Table 4 summarizes the optical characteristics of the PBS system. Figure 15 displays the RMS field map (i.e. Strehl Ratio map) on the focal plane image produced on CAM1 proving the high optical quality of the designed system (Strehl ratio greater than 97% in most of the image).

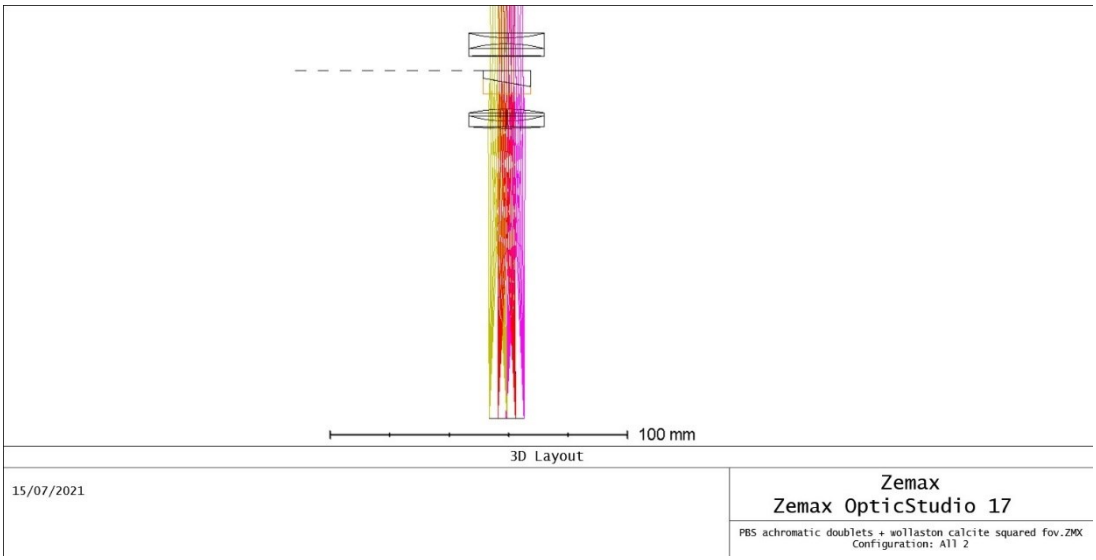

Figure 13: Wollaston prism made of calcite inserted in the collimated beam between the two corrective achromatic doublets.

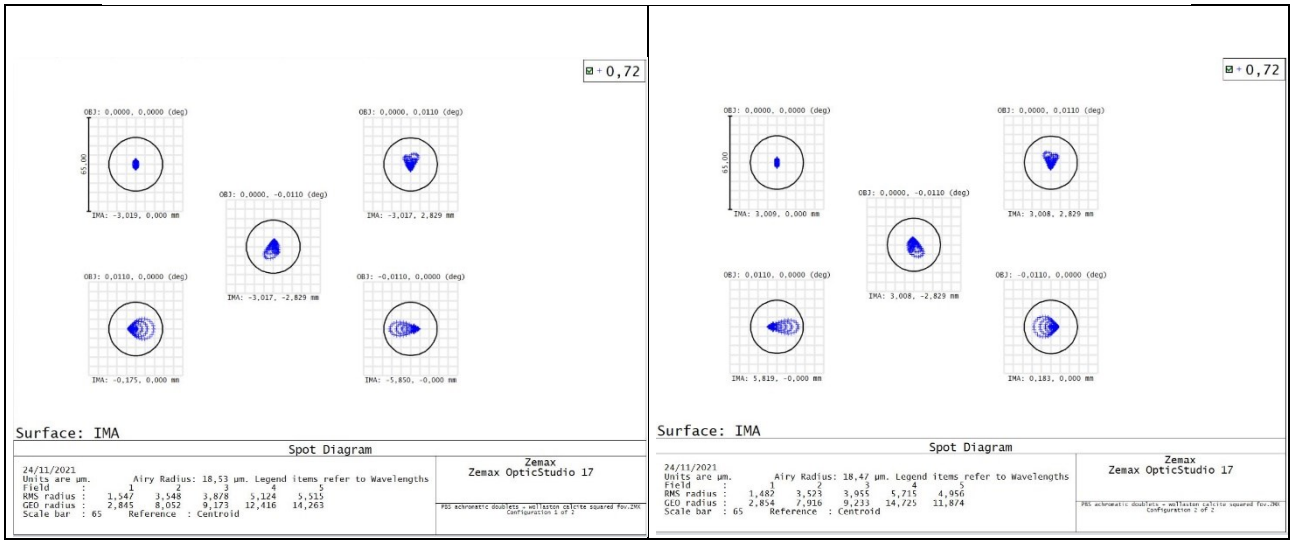

Figure 14: Spot diagrams at 720.0 nm of both the split beams by the Wollaston prism made of calcite placed in the collimated beam between the two corrective achromatic doublets.

Negative achromatic doublet	Thorlabs ACN254-100-A (with suitable custom AR coating in the wavelength range 580-860 nm)
Positive achromatic doublet	Thorlabs AC254-100-A (with suitable custom AR coating in the wavelength range 580-860 nm)
Wollaston prism cutting angle [°]	10
Wollaston prism dimensions [mm]	16 (squared)
Wollaston prism length [mm]	8
Beam splitting angle at 720 nm [°]	3.4876
Distance between the two split images' centers (wavelength range 580-860 nm) [mm]	6.07-6.08
Single image dimension in spectro-polarimetric mode (wavelength range 580-860 nm) [mm]	5.66-5.60
Length of the PBS system [mm]	~ 32
Position of the first optical surface of the PBS system from the CAM1 sensor at 720 nm [mm]	~ 129
Focus shift of CAM1 without and with the PBS system [mm] at 580 nm	28.371
Chromatism (wavelength range 580-860 nm) without PBS system [mm]	4.640
Chromatism (wavelength range 580-860 nm) with PBS system [mm]	4.589
CAM1 total travel (focus shift + chromatism) [mm]	32.96
Overall image dimension on CAM1 (wavelength range 580-860 nm) [mm]	11.723-11.711
Distance between the two central edges of the split images (wavelength range 580-860 nm) [mm] / [pixel]	0.378-0.430 / 58-66
Distance between the external edges of the split images and the edge of the CAM1 sensor [pixel]	~ 120

Table 4: Optical characteristics of the PBS system with a calcite Wollaston prism and two achromatic doublets.

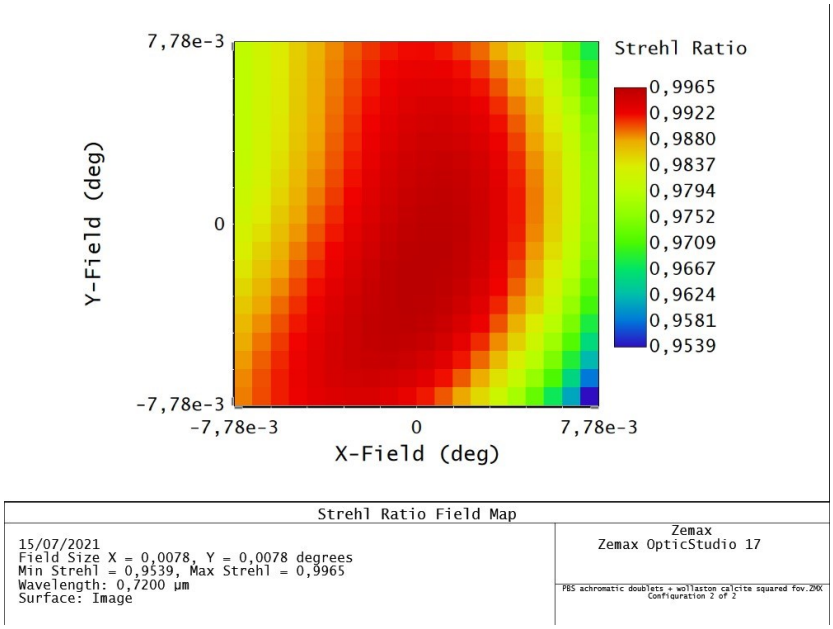

Figure 15: RMS Field Map of the PBS system with a calcite Wollaston prism and two achromatic doublets.

Singlets design

Figure 16 shows the corrective lens system based on two singlets glued (to reduce ghosts) with the Wollaston prism made of calcite designed with OpticStudio to fit the IBIS 2.0 PBS requirements. Figure 17 shows the two spot diagrams at 720.0 nm (in the middle of the IBIS 2.0 spectral range) produced by this PBS system (diffraction limited, spots inside the Airy disks). Similar spot diagrams are obtained over the whole spectral range of 580-860 nm. Table 5 summarizes the optical characteristics of the PBS system. Figure 18 displays the RMS field map (i.e. Strehl Ratio map) on the focal plane image produced on CAM1 proving the high optical quality of the designed system (Strehl ratio greater than 95% in most of the image).

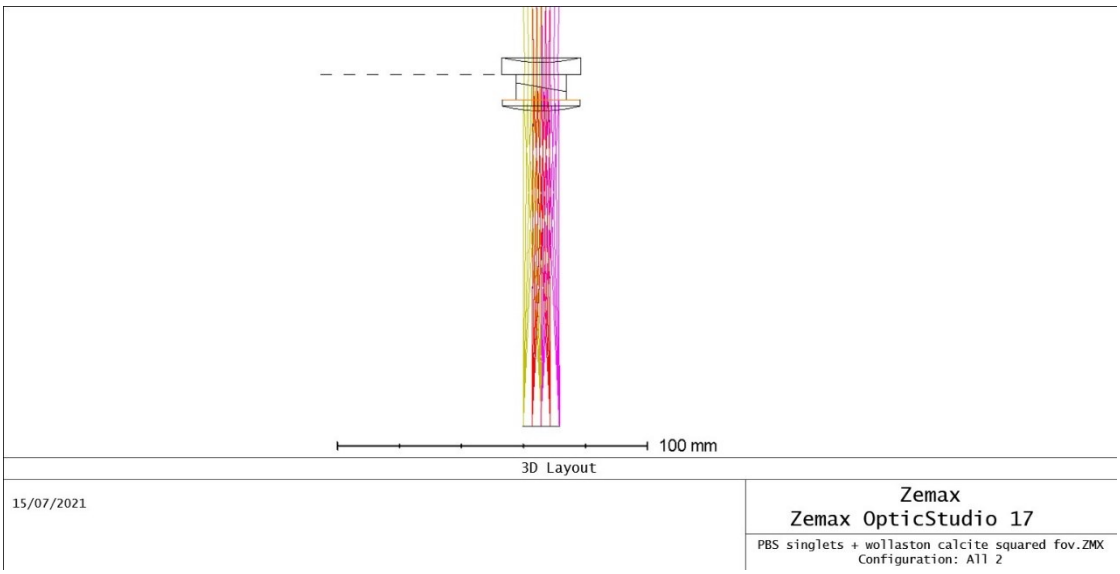

Figure 16: Wollaston prism made of calcite inserted (in contact) in the collimated beam between the two corrective singlets.

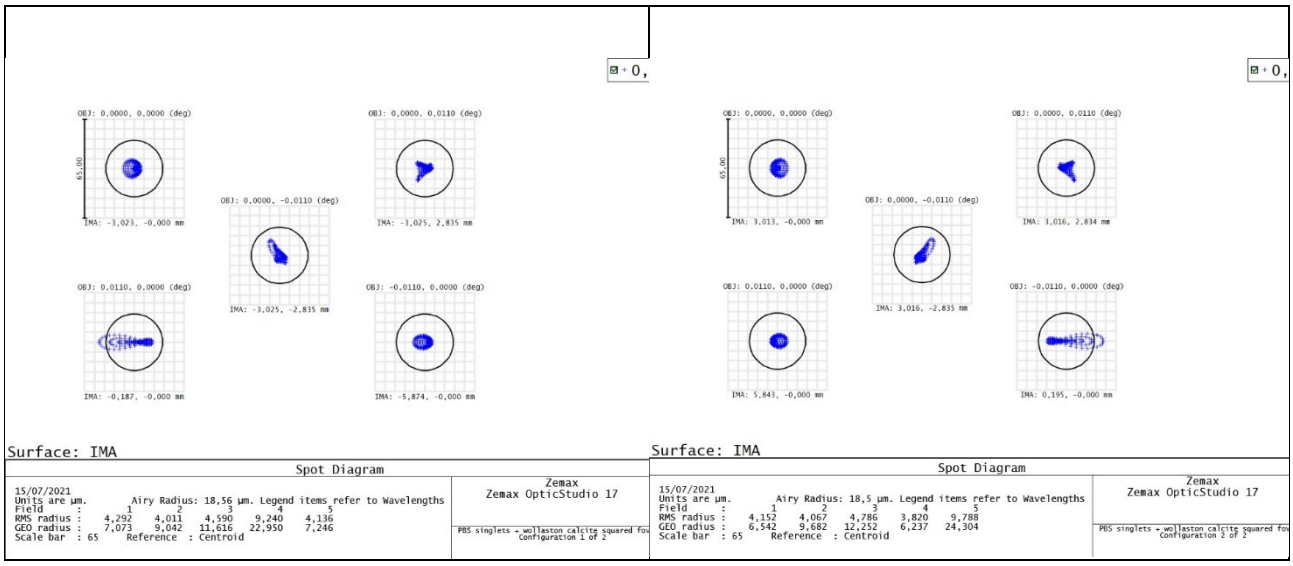

Figure 17: Spot diagrams at 720.0 nm of both the split beams by the Wollaston prism made of calcite placed in the collimated beam between the two corrective singlets.

Negative singlet	Thorlabs LC1120 (with suitable custom AR coating in the wavelength range 580-860 nm)
Positive singlet	Thorlabs LA1251 (with suitable custom coating AR in the wavelength range 580-860 nm)
Wollaston prism cutting angle [°]	10
Wollaston prism dimensions [mm]	16 (squared)
Wollaston prism length [mm]	8
Beam splitting angle at 720 nm [°]	3.4876
Distance between the two split images' centers (wavelength range 580-860 nm) [mm]	6.08-6.10
Single image dimension in spectro-polarimetric mode (wavelength range 580-860 nm) [mm]	5.66-5.64
Length of the PBS system [mm]	~ 18
Position of the first optical surface of the PBS system from the CAM1 sensor at 720 nm [mm]	~ 119
Focus shift of CAM1 without and with the PBS system [mm] at 580 nm	15.504
Chromatism (wavelength range 580-860 nm) without PBS system [mm]	4.640
Chromatism (wavelength range 580-860 nm) with PBS system [mm]	4.644
CAM1 total travel (focus shift + chromatism) [mm]	20.1
Overall image dimension on CAM1 (wavelength range 580-860 nm) [mm]	11.818-11.818
Distance between the two central edges of the split images (wavelength range 580-860 nm) [mm] / [pixel]	0.410-0.466 / 63-72
Distance between the external edges of the split images and the edge of the CAM1 sensor [pixel]	~ 114

Table 5: Optical characteristics of the PBS system with a calcite Wollaston prism and two singlets.

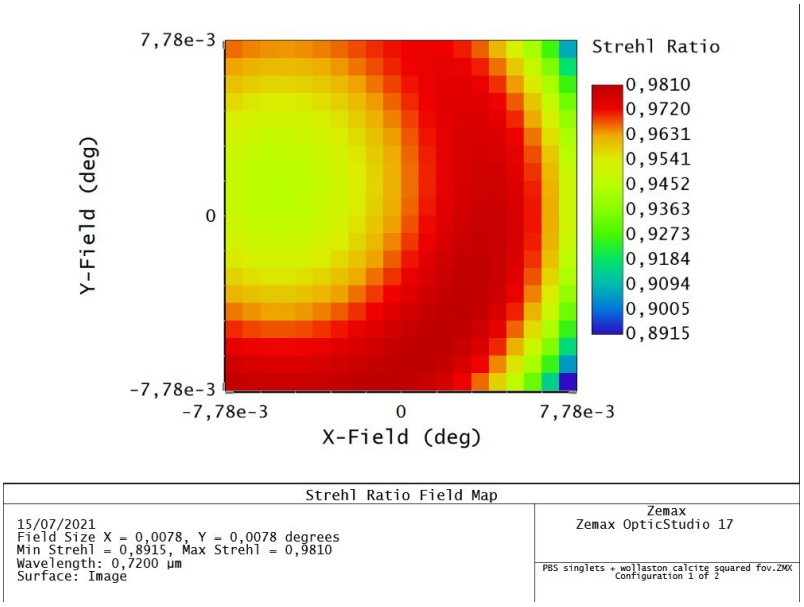

Figure 18: RMS Field Map of the PBS system with a calcite Wollaston prism and two singlets.

7 LCVRs optical quality characterization

In the framework of the design study, an optical quality characterization of a LCVR produced by Thorlabs (model LCC1111-B, free aperture of 10 mm) was also performed. The tested component is available in the Optical Laboratory of the INAF – Astronomical Observatory of Rome with its benchtop controller. The optical characterization has been carried out at the Optical Laboratory of the INAF – Astrophysical Observatory of Arcetri. The optical test aimed to characterize the optical quality of the LCVRs produced by Thorlabs, since it is a critical parameter due to the LCVRs position at 150-200 mm from the pupil plane between the two relay lenses; the other specifications are in accordance with the instrumental requirements, with few custom modifications.

The instrument used to perform the optical quality characterization was a WYKO RTI 4100 laser interferometer (https://www.bruker.com/en.html). The optical setup with the LCVR placed between the interferometer and a reference flat mirror (LCVR in double pass) is shown in Figure 19. The LCVR has been characterized with no voltages (maximum retardance, approximately 1.15λ, OFF), with a retardance of λ/4 (quarter-wave plate, QWP) and with a retardance of λ/2 (half-wave plate, HWP).

The raw data have been fitted in order to remove the low order Zernike polynomials: piston, tip-tilt and power. The standard deviations of the optical surface of the LCVR in OFF, QWP and HWP mode are 4.9 nm, 5.0 nm and 5.0 nm, respectively. The optical quality maps are reported in Figure 20 in units of nanometer surface (rescaled for single pass, therefore the aberration introduced by the LCVR). This optical characterization shows that the LCVRs by Thorlabs have a suitable optical quality for the IBIS 2.0 polarimeter. In addition, only very few pattern differences on the optical quality are introduced by the retardances (voltages) variations.

Figure 19: Optical setup used for the optical quality characterization of a LCVR produced by Thorlabs: WYKO RTI 4100 laser interferometer, the LCVR with its benchtop controller and a reference flat mirror.

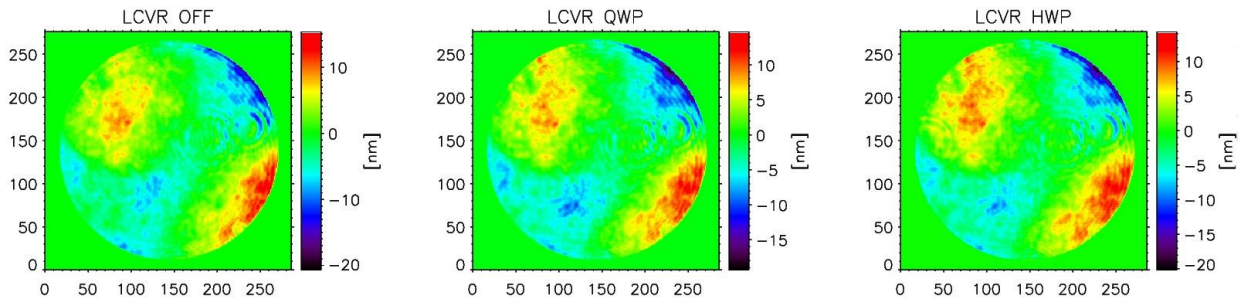

Figure 20: Optical quality maps of the LCVR in OFF, QWP and HWP mode.

8 Conclusions

In this document, the conceptual design of the IBIS 2.0 polarimetric unit has been presented. After describing the design of the previous polarimeter used with IBIS at DST, several alternatives have been described for the polarimeter of IBIS 2.0, by considering both the optical components and the modulation strategies. For several discussed reasons the IBIS 2.0 polarimeter has been designed using the IBIS polarimeter at DST as a model during a reverse engineer process combined with a more modern design performed with OpticStudio software. The design has been also validated with dedicated routines developed in IDL.

The polarimetric modulator of IBIS 2.0 will be realized with two LCVRs mounted with their axis at 90° and 135° respectively and switched in 6 modulation states. Their voltages calibration will be performed using a calibration linear polarizer with its axis alternatively set at 90° and 45° for the calibration of the LCVR 2 and the LCVR 1, respectively. The IBIS 2.0 X-matrix will be evaluated inserting the ICU of the VTT in the beam coming from the telescope and switching its retarder and its polarizer in 16 configurations.

The polarimetric analyzer of IBIS 2.0 will by a PBS realized with a Wollaston prism made of calcite and a corrective lenses system. Two different designs for the corrective lenses system have been optimized and presented, based on two achromatic doublets or two singlets cemented with the Wollaston prism.

Finally, our conceptual design has been integrated with an optical quality characterization of an LCVR produced by Thorlabs available in the Optical Lab of the INAF-OAR, proving that the LCVRs produced by this vendor have an optical quality which is adequate for the IBIS 2.0 polarimeter.

Table 6 resumes the instrumental requirements of the IBIS 2.0 polarimeter, the analyzed alternatives and the achieved values during the design, all of which meet all requirements.

Item	Requirements	Alternatives	Achieved
FoV [arcsec^2]	80x80	80x80 or 80x40	80x80
Distance between the two split images' centers [mm]	6.65	-	6.08 (PBS doublets) – 6.09 (PBS singlets) No split images overlapping (see Table 4 and Table 5)
Single image dimension in spectro-polarimetric mode [mm]	5.69	-	5.63 (PBS doublets) – 5.63 (PBS singlets)
Beam diameter in the polarimetric modulator place [mm]	< 50	-	~ 15
Available space for the PBS (LxWxH) [mm]	45x18x18	-	32x16x16 (doublets) or 18x16x16 (singlets)
Polarimetric Modulators	-	LCVRs, FLCs	LCVRs
Number of modulation states	-	6, 4	6
Polarimetric Analyzer	-	Wollaston prism, Modified Savart Plate, set of cemented polarizing cube beam splitters, single polarizing cube beam splitter	Wollaston prism
PBS crystal type	-	Calcite, Quartz	Calcite
Orientation angle of the LCVRs	-	All	90° for LCVR1 and 135° for LCVR2
Orientation angle of the calibration linear polarizer	-	All	45° for LCVR1 (with LCVR2 set at λ/4) and 90° for LCVR2 (with LCVR1 set at 0λ)
X-matrix	-	-	16 configurations of the ICU
T-matrix	-	-	*vtt.pro* code and measurements

Table 6: Instrumental requirements of the IBIS 2.0 polarimeter, the analyzed alternatives and the achieved values during the design.

Appendix A: Scientific bibliography

C. Beck (2002), The calibration of the vector polarimeter POLIS (Diploma Thesis)

C. Beck et al. (2005a), A&A, 437, 1159-1167

C. Beck et al. (2005b), A&A, 443, 1047-1053

C. Beck et al. (2010), A&A, 520, A115

N. Bello Gonzalez and F. Kneer (2008), A&A, 480, 265-275

C. Capitani et al. (1989), Solar Physics, 120, 173C

F. Cavallini (2006), Solar Physics, 236, 415-439

M. Collados (1999), ASP Conf. Ser., 184, 3C

M. Collados (2007a), Modern Solar Facilities, Univ. Gottingen, 143-150

M. Collados et al. (2007b), ASP Conference Series, 368

J. C. del Toro Iniesta and M. Collados (2000), Applied Optics, 39, 10

J. C. del Toro Iniesta (2003), Introduction to Spectropolarimetry, Cambridge University Press

A. M. Gandorfer (1999), Optical Engineer, 38 (8), 1402-1408

C. U. Keller, Instrumentation for Astrophysical Polarimetry, Leinden University Class Notes

B. W. Lites (1987), Applied Optics, 26, 18

V. Martinez Pillet et al. (1999), ASP Conf. Ser., 183, 264M

K. G. Puschmann et al. (2012), Astron. Nachr., 9, 880-893

G. Scharmer (2006), A&A, 447, 1111-1120

W. Schmidt et al. (2001), ASP Conf. Ser., 236, 49S

W. A. Schurcliff (1962), Polarized Light, Harvard Univ. Press

O. van der Luhe et al. (2003), SPIE, 4853, 187V

--- End of document ---